Macromolecular Research, Vol. 23, No. 10, pp 971-976 (2015)
DOI 10.1007/s13233-015-3121-2

www.springer.com/13233
pISSN 1598-5032 eISSN 2092-7673

Morphology and Mechanical Properties of Polyketone Blended with Polyamide and Ethylene-Octene Rubber

Yongho Kim[1], Jin Woo Bae[1], Choon Soo Lee[2], Sunghun Kim[1], Hogun Jung[1], and Jae Young Jho*,[1]

[1]School of Chemical and Biological Engineering, Seoul National University, Seoul 151-744, Korea
[2]Polymeric Materials Research Team, Hyundai Motor Group R&D Division, Hwaseong, Gyeonggi 445-706, Korea

Received July 3, 2015; Revised July 7, 2015; Accepted July 8, 2015

Abstract: To enhance impact strength of polyketone (PK), maleic anhydride-grafted ethylene-octene rubber (mEOR) was blended via melt mixing. Nylon 6 (PA6) was employed as the third component to compatibilize PK/mEOR blends. The changes in mechanical properties, morphology, and fracture behavior of the blends by the addition of PA6 were investigated. PK was not toughened by mEOR alone, as the binary blends had lower elongation at break and similar impact strength compared with those of PK. The addition of PA6 gave rise to increases in impact strength as well as in tensile properties, exhibiting the compatibilizing effect of PA6. The lowered interfacial tension was confirmed by the phase morphology, in which PA6 encapsulated mEOR particles of reduced sizes. The observation of sub-surface damage zone also indicated that the toughening of PK by mEOR rubber was effective in the presence of PA6.

Keywords: polyketone, ethylene-octene rubber, blend, compatibilizer, polyamide.

Introduction

Aliphatic polyketone (PK) is a terpolymer consisting of carbon monoxide, ethylene, and a small amount of propylene as the comonomers. As an engineering plastic PK is often compared to nylon 6 (polyamide 6, PA6). While PK is more competitive in some properties including chemical resistance and barrier property, mechanical properties of the two polymers are comparable.[1-3] Taking advantage of these properties, PK is exploiting the areas of application as engineering or packaging material. As PK becomes brittle in the presence of notch or defect, just like other polymers, toughening of the polymer is necessary for engineering applications.[4]

The efforts of toughening PK have been made in two directions; copolymerization and blending. It has been reported that a PK terpolymer with a few mole percent of alpha olefins as the third monomers had an enhanced notched impact strength with a lower ductile-brittle transition temperature.[5] The enhanced impact strength has appeared to be a result of the lowered crystallinity. However, only propylene has been effective in giving desired balance of crystallinity and property. For the copolymers with a larger olefin like hexylene the decrease in crystallinity, yield strength, and tensile strength, which accompanied the increase in impact strength, appeared to be excessive. The commercial PK is usually produced with a few mole percent of propylene.

As another approach to enhance impact strength of PK, a variety of polymers has been blended with PK. The polymer ranges from rigid ones like polyurethane, amorphous PA, PA6, and PA6/high density polyethylene to rubbery ones like copolyester (Hytrel®), core-shell rubber, and ethylene-methacrylic acid copolymer (Surlyn®).[6-13] The extent of increase in impact strength in these blends, however, appeared not as large as expected even in the blends with rubbers. The main reason for this has been attributed to poor adhesion between the phases. It was observed in a calcium carbonate composite of PK that impact strength as well as flexural strength was enhanced, when rigid calcium carbonate particles were coated with stearic acid for good interface.[14] In a very recent effort CO and ethylene were copolymerized in situ on the powdered rubber in the presence of an apolar solvent, which resulted in some improvement in interfacial adhesion between PK and rubber.[15]

In the present study, we are to report the use of a rubber, maleic anhydride-grafted ethylene-octene rubber (maleated EOR, mEOR), as a modifier to enhance the impact strength of PK. Compared with other olefin copolymers like ethylene-propylene rubbers (EPR) or ethylene-propylene-diene terpolymers (EPDM), mEOR is of better-defined structure and narrower molecular weight distribution, which have been known to be beneficial for impact modification.[16,17] While the mechanical properties of polymer blends are directly affected by the quality of the interphase, the interphase between PK and mEOR is not expected to be fair enough to give enhanced impact strength.[18-20] We selected PA6 as a polymer compatibilizer for the blends of this study, as PA6 was considered to interact

*Corresponding Author. E-mail: jyjho@snu.ac.kr

with both of PK and mEOR. It has been reported that a reactive compatibilization between PA6 and mEOR occurred during the melt compounding.[16,17] It has also been reported that PA6 is partially compatible with PK through the formation of hydrogen bonding.[9,21,22] Through the measurement of mechanical properties and the observation of fracture surface and sub-surface morphology, the effectiveness of mEOR and PA6 as an impact modifier and a compatibilizer for PK is investigated.

Experimental

Materials and Preparation. PK terpolymer containing 6 mol% of propylene used in this study was kindly supplied by Hyosung. PA6 was also obtained from Hyosung under the trade name of 1011BRT. mEOR was purchased from DuPont Dow Elastomers under the trade name of Fusabond MN493D.

All materials were used without any purification except drying at 60 ºC for 24 h in a vacuum oven prior to blending. The blends were obtained using a co-rotating twin screw extruder (Hankook E.M., STS 32HS). The diameter and length-to-diameter ratio of the screw were 32 and 36 mm, respectively. The temperature profiles in the extruder were 210-230 ºC from hopper to die zone, and the screw rotating speed used was 200 rpm. The extruded blends were water-cooled, pelletized, and dried.

The blends were coded with letters and numbers. The numbers after the letter K and A referred to the weight fraction of PK and PA6, respectively, and that after hyphen to the content of mEOR in phr. For example, K7A3-5 was composed of 70 wt% of PK, 30 wt% of PA6, and 5 phr of mEOR.

Characterization and Measurement. Morphology was investigated with a field emission scanning electron microscope (FE-SEM, JEOL, JSM-6701F). To investigate the phase morphology, specimens were fractured under cryogenic conditions using liquid nitrogen. The phases of mEOR and PA6 were etched with hexane and formic acid for 1 h, respectively, when needed. For the rubber phase size and size distribution determination, SEM micrographs were analyzed by using Image Pro Plus 6.2 software. Through the appropriate calculations the number-average, weight-average diameters, and size distribution were determined. Morphology was examined also with a transmission electron microscope (TEM, Carl Zeiss, LIBRA 120). The samples were prepared by microtoming at -100 ºC using a cryo-ultramicrotome (RMC Products, PT-PC PowerTome), followed by transfer onto carbon-coated Cu grids of 200 mesh. The samples were stained by the vapors of RuO_4 (0.5 wt% in water, Acros Organics) for PA6 or OsO_4 (4 wt% in water, Sigma-Aldrich) for mEOR phase.

The test specimens for measuring tensile properties and impact strength were prepared using an injection-molding machine (Engel, Victory 650/150). Young's modulus and yield stress were determined using a universal testing machine (Zwick/Roell, Z010) at 25 ºC and at the crosshead speed of 50 mm/min according to ASTM D-638 Type I method, which is for the specimen of 127 × 12.7 × 6.4 mm^3 in dimension. The notched Izod impact strength of the specimens was measured using an impact tester (Yasuda, PC-S) in accordance with ASTM D-256 at 25 ºC, which is for the specimen of 63.5 × 12.7 × 6.4 mm^3 in dimension with a 2.54-mm notch depth and 45º notch angle.

The double-notch four-point-bend (DN-4PB) tests were conducted with the rectangular bars of 63.5 × 12.7 × 6.4 mm^3 in dimension. The specimens were notched with Tinius Olsen Model 899 specimen notcher, followed by razor blade tapping to open a sharp crack with a parabolic crack front. The schematic representation of the test configuration has been reported elsewhere.[23-25] Under loading, one crack breaks while the other is arrested before fracture. The sub-surface damage zones near arrested crack tip of the DN-4PB specimens were observed using transmitted light optical microscopy (TOM).

Results and Discussion

Morphology. As mechanical properties of rubber-toughened polymers should be dependent on the state of rubber phase including particle size as well as the rubber content, morphology of the blends was examined. Figure 1 showed the cryofractured surfaces of K-10 and K7A3-10. The surface of K-10 (Figure 1(a)) revealed the typical morphology of an immiscible blend with large and polydisperse spherical mEOR particles in PK matrix, which was a result of high interfacial tension and coalescence. It was also observed that some of the mEOR particles had been removed during the fracture process, leaving smooth and clean marks, due to the lack of interfacial adhesion. Fracture surface of K7A3-10 was markedly different from that of K-10; the rubber phase structure was not distinguishable, and detachment at the interface was not observed (Figure 1(b)). Figure 1(c) showed the surface of the same blend after the mEOR phase had been extracted by etch-

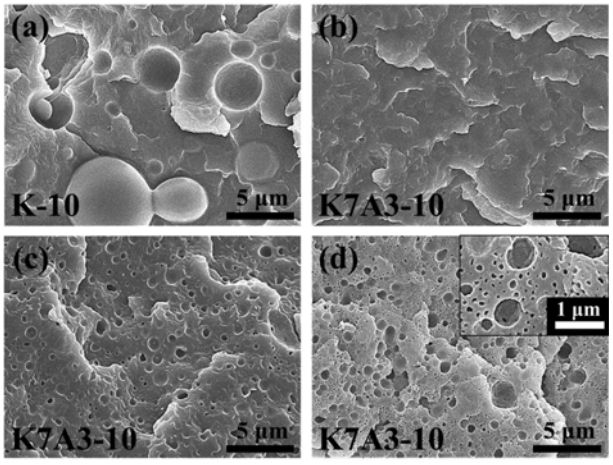

Figure 1. SEM images of the cryofractured surface of (a) K-10, (b) K7A3-10, (c) K7A3-10 after mEOR phase extracted, and (d) K7A3-10 after mEOR and PA6 phases extracted.

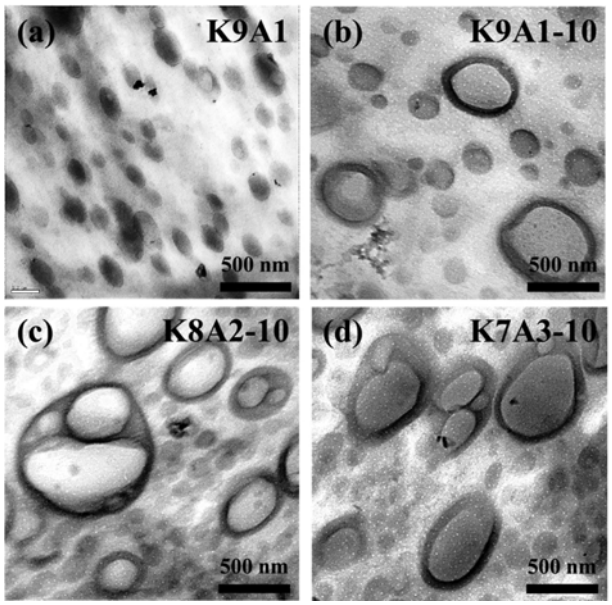

Figure 2. TEM images of (a) K9A1, (b) K9A1-10, (c) K8A2-10, and (d) K7A3-10. PA6 and mEOR phases were stained with RuO_4 and OsO_4, respectively. Grey mEOR and darker grey PA6 phases were dispersed in white PK matrix.

ing with hexane. Compared with K-10 a finer dispersion of submicron-sized domains was observed, which indicated the effective compatibilization of added PA6. When the hexane-treated (mEOR-removed) sample was further treated with formic acid, the surface revealed a still finer dispersion of PA6 domains with tens of nanometers in diameter (Figure 1(d)).

The TEM images in Figure 2 provided a more detailed view of the phase morphology of the blends. Figure 2(a) showed the dark grey PA6 phase dispersed in the white PK matrix in K9A1 binary blend. Figure 2(b)-(d) showed the morphology of the ternary blends containing 10 phr of mEOR and varying amount of PA6. In K9A1-10 the large grey particles of mEOR appeared to be encapsulated by PA6 shell, forming core-shell structure. Size of the mEOR particles agreed with that observed in SEM of Figure 1. This structure demonstrated that PA6 resided between PK and mEOR, reduced interfacial tension, and stabilized the resultant multiphase morphology. The microstructure became more complex in the blends with higher PA6 contents; PA6 interlayer thickened, and so-called 'salami' structure appeared. The formation of salami-like dispersed phase has been known to be very effective in toughening plastics, since it made the crack path complex and tortuous.[28,29] This additional effect, however, was not evident in the blends of this study, presumably due to the large size of the rubber particles and the non-prevalence of the salami structure.

From the morphology observed the following compatibilizing effect of PA6 was conjectured. The amine end groups of PA6 reacted with maleic anhydride group of mEOR to form mEOR-*g*-PA6 copolymer,[16,17] which compatibilized mEOR and PA6. On the other hand, the added PA6 itself resided between and compatibilized the PK and mEOR phases.

Table I. Particle Diameter and Size Distribution of mEOR Rubber in the Blends

Matrix	Rubber Content (phr)	d_n (μm)	d_w (μm)	d_w/d_n
PK	5	2.10	2.72	1.30
	10	2.72	3.94	1.45
	15	5.25	7.52	1.43
K9A1	5	0.55	0.66	1.21
	10	0.54	0.68	1.27
	15	0.57	0.73	1.27
K8A2	5	0.31	0.38	1.21
	10	0.32	0.40	1.26
	15	0.32	0.41	1.28
K7A3	5	0.27	0.32	1.19
	10	0.30	0.36	1.20
	15	0.29	0.36	1.24

Particle size and size distribution was determined by analyzing the SEM micrographs using a software and listed in Table I. In the binary blends of PK/mEOR, as the content of rubber increased, both of the number- (d_n) and weight-average (d_w) particle size increased, and the size distribution broadened. As PA6 was added there were sharp drop in the size and size distribution of mEOR particles. As the rubber content increased in these blends there were only small increases in particle size and nominal broadening in size distribution. The fine dispersion of a dispersed phase upon incorporation of a compatibilizer is caused by a decrease in interfacial tension and coalescence. In a study evaluating the relative role of interfacial tension and coalescence in determining the domain size of the dispersed phase, lowering of interfacial tension and suppression of coalescence were determined equally important.[30] It was therefore believed that PA6 in the blends of this study was efficient in compatibilizing the PK/mEOR blends by lowering the interfacial tension and stabilizing the morphology against coalescence. The effectiveness of PA6 as the compatibilizer was also manifested by the sharp increase in impact strength with the addition of PA6, as discussed in the next section. The concurrence of the decrease in particle size and the increase in impact strength was considered natural, as the particle size should be one of the most important factor determining the toughness or impact strength of polymer blends.

Mechanical Properties. The results of the tensile and Izod impact tests were summarized in Figure 3. Young's modulus and yield stress of PK decreased with the addition of mEOR. The decreases were usual considering the elastomeric nature of the mEOR and the positive proportionality between Young's modulus and yield strength. On the other hand, Young's modulus

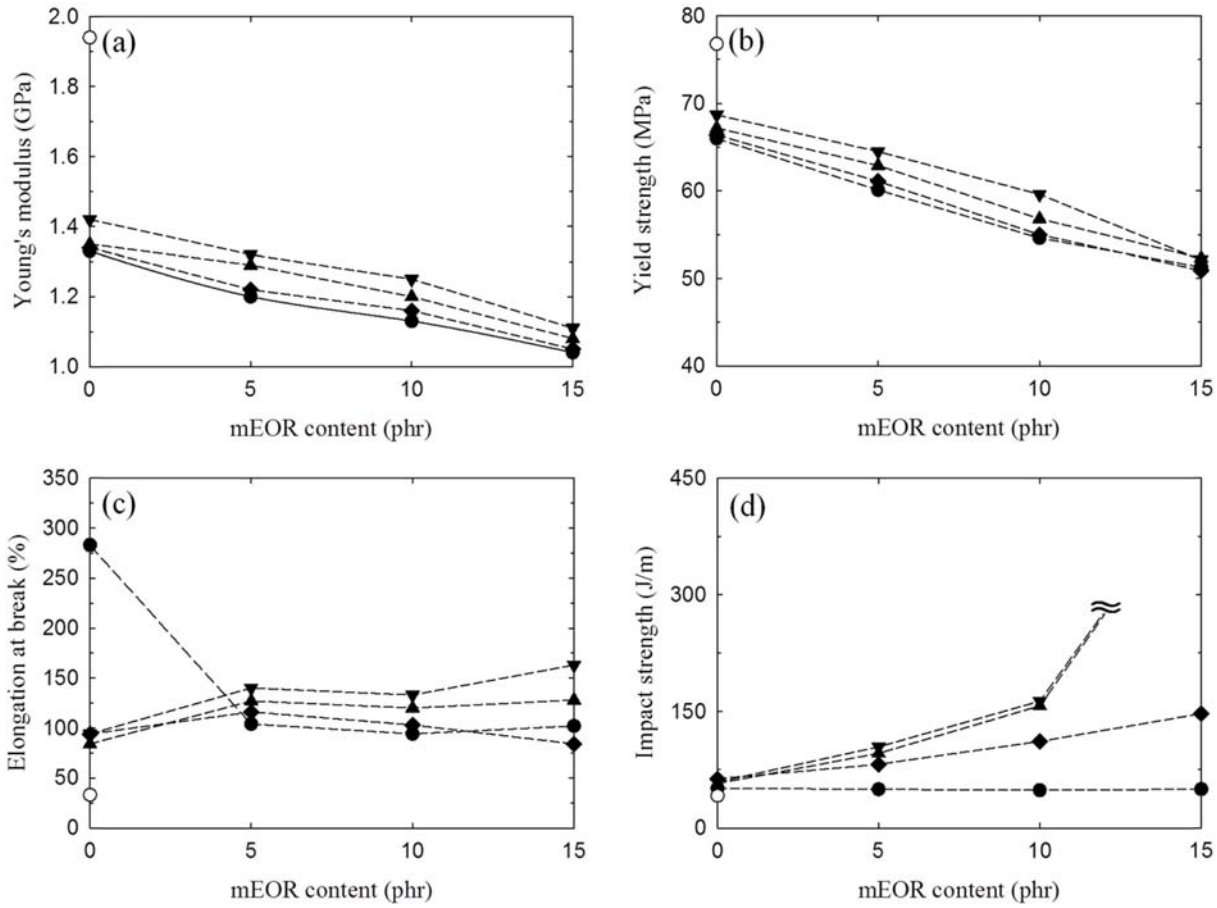

Figure 3. (a) Young's modulus, (b) yield stress, (c) elongation at break, and (d) notched Izod impact strength of PK and its blends as a function of mEOR content. ● PK; ◆ K9A1; ▲ K8A2; ▼ K7A3; ○ PA6. Note that K8A2 and K7A3 with 15 phr of mEOR did not break at the impact test condition.

and yield stress were higher for the blends with higher PA6 content at the same rubber content, which were the consequence of the higher Young's modulus and yield stress of the PA6 than those of PK.

The elongation at break data had relatively large standard deviations, which made it difficult to describe a clear trend. It was partly because that many factors affect the elongation at break of a material, including impurities, defects, and testing rate, in addition to intrinsic structure and morphology. One thing apparent was that the PK/mEOR blends had lower elongation at break than PK, despite the addition of an elastomer. The reason for this was considered to be the poor interfacial adhesion between PK and mEOR; large rubber particles gave weak points and initiated breaking when the tensile force was applied. It was reported that when EOR particles were larger than about 1 μm, the particles cavitated and initiated crazes, which then caused premature rupture.[26] The other thing also apparent was that elongation at break of the PK/mEOR blend increased with the addition of PA6. This was attributed to the improved interfacial adhesion between PK and mEOR.

The result of impact test exhibited more evidently the role of PA6 as the polymer compatibilizer. By the addition of mEOR rubber only, impact strength of the blends did not increase from that of PK. The similar results were observed when EOR was blended with amorphous or semicrystalline PA6, where interfacial adhesion was poor.[26,27] When PA6 was added as the third component of the blends, impact strength increased with increasing content of PA6 as well as with increasing content of the rubber. The degree of enhancement in impact strength of the blends was substantial, and the blends containing 20 or 30 wt% of PA6 toughened with 15 phr of mEOR did not break under the current impact test condition. The effective toughening of PK with mEOR and PA6 combined was considered to be the result of the formation of PA6-*g*-mEOR copolymer, which acted as a compatibilizer improving interfacial adhesion as mentioned above.

Toughening Mechanism. As the appearance of fracture surface might reflect the fracture process, the impact-fracture surfaces of PK and the blends were examined. As shown in Figure 4, each of the fracture surfaces had a slow-crack-growth region next to the notch root and a fast-crack-growth region

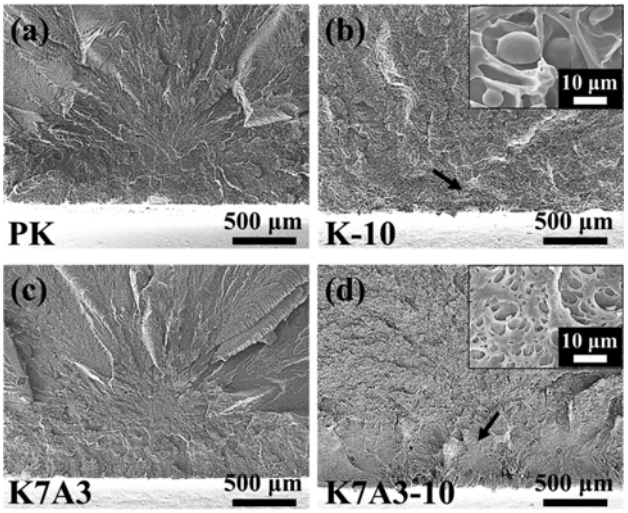

Figure 4. SEM images of impact-fractured surface of (a) PK, (b) K-10, (c) K7A3, and (d) K7A3-10. The crack propagated from bottom to top. Insets showed the magnified image of the slow crack growth regions (indicated by the arrows).

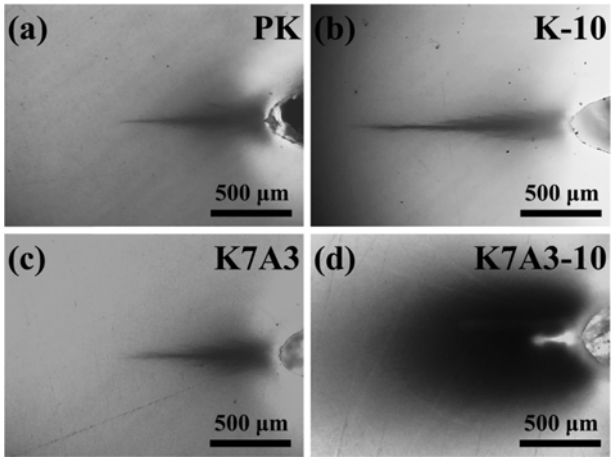

Figure 5. TOM images of unbroken notch of the DN-4PB tests of (a) PK, (b) K-10, (c) K7A3, and (d) K7A3-10. The crack propagated from right to left.

with half-radial propagation markings. The distinction between slow- and fast-crack-growth regions in the fractograph of PK was rather clear; the former was rough and the latter was smooth (Figure 4(a)). The surface of K-10 (PK with 10 phr mEOR) was different from that of PK in that the surface was 'sponge-like' with hemispherical holes all over the area, which made the surface look rough even in the fast-growth region. Under higher magnification (inset of Figure 4(b)) the debonded rubber particles and cavities were observed. Although debonding and cavitation themselves could absorb impact energy through causing larger and tortuous crack path, the amount of energy by these process appeared not large enough to enhance the impact strength over that of PK.[31] The poor interfacial adhesion between PK and mEOR and resultant large particle size appeared to make rubber toughening ineffective in this blend.[32]

The fracture surface of K7A3 shown in Figure 4(c) looked much alike that of PK. Although there should be PA6 particles of a few tens of nanometer in size dispersed in PK matrix, these particles appeared not toughen PK. It was considered that the particle size was smaller than the critical size that could toughen the matrix, and that the modulus mismatch between the phases was not large enough also. It has often been observed that particles smaller than the critical size were ineffective in toughening, regardless of whether it was the result of the compatibility of the phases or not.[26,27,33] The fracture surface of K7A3-10 shown in Figure 4(d) was much different from the above three. The feather-like markings characteristic of craze propagation was absent; instead, stress-whitening was observed. The inset fractograph exhibited extensive debonding and deformation of the matrix, which appeared the toughening mechanism of this blend. It is considered that the triaxial state of stress formed ahead of the notch was relieved by debonding at the interface, and shear yielding of the matrix was enabled to prevent the matrix from crazing.[14,24,32] In addition, the 'terrace' type of morphology was observed, in which the defected cracks were located at different layers. This type of 'crack deflection toughening' was considered to contribute to the high impact strength of this blend.[34]

The fracture behavior is more clearly demonstrated in Figure 5, which showed the TOM images of the sub-surface damage zone around the surviving crack tip of the DN-4PB specimens with the same blend composition to those of Figure 4. The dark damage zones were due to the light scattering by the cavities formed by the crack-opening stress. For PK, K-10, and K7A3, as expected, only small sub-surface damage zones were developed at the crack tip (Figure 5(a)-(c)), which indicated the lack of effective toughening mechanisms in these compositions.[35] It appeared that the presence of mEOR particles alone (K-10) or PA6 alone (K7A3) did not give rise to cavitation and/or debonding of particles, which could toughen the matrix PK. The damage zone of K7A3-10 ternary blend (Figure 5(d)) was much larger than those of the binary blends, which indicated the massive cavitation and/or debonding of rubber particles. In addition, the zone appeared to be consisted of two regions; the larger circular grey region and the darker elliptical region closer to the crack tip. It has been known that the contrast in darkness is due to the differences in the concentration and the extent of cavities as well as the amount of shear deformation within the two regions. The outer circular zone was considered to contain rubber particles that had cavitated due to the hydrostatic tension, and the inner darker zone to contain highly dilated cavities and shear bands.[23,36,37] The results above implied that the resistances to crack initiation and crack propagation of PK/mEOR blend were significantly enhanced by addition of PA6, thus better impact strength were expected in this blend, which again corresponded to the result of Izod impact strength test.

Conclusions

The binary blends of PK and mEOR had lower elongation at break and similar impact strength compared with those of PK, despite the addition of rubber. This ineffective toughening was due to the incompatibility of the phases, which gave large particles with poor interface. With the addition of PA6, impact strength as well as tensile properties of the blends were significantly enhanced. In ternary blends, rubber particles with reduced size were encapsulated by PA6 to form core-shell or salami structure. The size of plastic zone developed ahead of crack tip indicated that toughening was effective in the ternary blends. It was certain that PA6 worked as a compatibilizer in rubber-toughening of PK.

Acknowledgments. This research was supported by a grant from the Fundamental R&D Program for Technology of World Premier Materials funded by the Ministry of Trade, Industry, and Energy, Republic of Korea.

References

(1) M. A. Del Nobile, G. Mensitieri, and A. Sommazzi, *Polymer*, **36**, 4943 (1995).
(2) A. Sommazzi and F. Garbassi, *Prog. Polym. Sci.*, **22**, 1547 (1997).
(3) G. P. Belov and E. V. Novikova, *Russ. Chem. Rev.*, **73**, 267 (2004).
(4) W. C. J. Zuiderduin, J. Huétink, and R. J. Gaymans, *J. Appl. Polym. Sci.*, **91**, 2558 (2004).
(5) W. C. J. Zuiderduin, D. S. Homminga, J. Huétink, and R. J. Gaymans, *Polymer*, **46**, 1921 (2005).
(6) R. L. Danforth, W. P. Gergen, D. L. Handlin Jr, and R. G. Lutz, US Patent 4,851,482 (1989).
(7) W. P. Gergen and W. W. C. Hart, US Patent 4,960,838 (1990).
(8) A. Asano, M. Nishioka, Y. Takahashi, A. Kato, S. Hikasa, H. Iwabuki, K. Nagata, H. Sato, T. Hasegawa, H. Sawabe, M. Arao, T. Suda, A. Isoda, M. Mukai, D. Ishikawa, and T. Izumi, *Macromolecules*, **42**, 9506 (2009).
(9) W. P. Gergen, J. M. Machado, D. G. Waters, and R. P. Gingrich, US Patent 5,043,389 (1991).
(10) W. P. Gergen, US Patent 4,818,798 (1989).
(11) W. C. J. Zuiderduin, D. P. N. Vlasveld, J. Huétink, and R. J. Gaymans, *Polymer*, **45**, 3765 (2004).
(12) W. C. J. Zuiderduin, D. P. N. Vlasveld, J. Huétink, and R. J. Gaymans, *Polymer*, **46**, 10321 (2005).
(13) W. P. Gergen and R. G. Lutz, US Patent 5,071,916 (1991).
(14) W. C. J. Zuiderduin, J. Huétink, and R. J. Gaymans, *Polymer*, **47**, 5880 (2006).
(15) R. Sulcis, F. Vizza, W. Oberhauser, F. Ciardelli, R. Spiniello, N. T. Dintcheva, and E. Passaglia, *Polym. Adv. Technol.*, **25**, 1060 (2014).
(16) S.-L. Bai, G.-T. Wang, J.-M. Hiver, and C. G'Sell, *Polymer*, **45**, 3063 (2004).
(17) K. Premphet-Sirisinha and S. Chalearmthitipa, *Polym. Eng. Sci.*, **43**, 317 (2003).
(18) S. Wu, *J. Polym. Sci. Polym. Phys. Ed.*, **21**, 699 (1983).
(19) S. Wu, *Polymer*, **26**, 1855 (1985).
(20) D. Dompas, G. Groeninckx, M. Isogawa, T. Hasegawa, and M. Kadokura, *Polymer*, **35**, 4760 (1994).
(21) D. Sémeril, E. Passaglia, C. Bianchini, M. Davies, H. Miller, and F. Ciardelli, *Macromol. Mater. Eng.*, **288**, 475 (2003).
(22) A. Kato, M. Nishioka, Y. Takahashi, T. Suda, H. Sawabe, A. Isoda, O. Drozdova, T. Hasegawa, T. Izumi, K. Nagata, S. Hikasa, H. Iwabuki, and A. Asano, *J. Appl. Polym. Sci.*, **116**, 3056 (2010).
(23) D. S. Parker, H.-J. Sue, J. Huang, and A. F. Yee, *Polymer*, **31**, 2267 (1990).
(24) H.-J. Sue and A. F. Yee, *J. Mater. Sci.,* **28**, 2975 (1993).
(25) R. A. Pearson, H.-J. Sue, and A. F. Yee, in *Toughening of Plastics*, American Chemical Society, Washington DC, 2000, pp 6-9.
(26) J. J. Huang, H. Keskkula, and D. R. Paul, *Polymer*, **47**, 639 (2006).
(27) J. J. Huang and D. R. Paul, *Polymer*, **47**, 3505 (2006).
(28) W. F. Yang and Y. Z. We, *Mater. Chem. Phys.*, **15**, 505 (1986).
(29) W. dong, X. Cao, and Y. Li, *Polym. Int.*, **63**, 1094 (2014).
(30) P. Cigana, B. D. Favis, and R. Jerome, *J. Polym. Sci.*, *Part B: Polym. Phys.*, **34**, 1691 (1996).
(31) J. Wu, Y.-W. Mai, and A. F. Yee, *J. Mater. Sci.,* **29**, 4510 (1994).
(32) Z.-Z. Yu, M. Lei, Y. Ou, and G. Yang, *Polymer*, **43**, 6993 (2002).
(33) A. J. Oshinski, H. Keskkula, and D. R. Paul, *Polymer*, **33**, 268 (1992).
(34) H.-J. Sue, *Polym. Eng. Sci.*, **31**, 275 (1991).
(35) G.-X. Wei, H.-J. Sue, J. Chu, C. Huang, and K. Gong, *J. Mater. Sci.,* **35**, 555 (2000).
(36) S.-C. Wong and Y.-W. Mai, *Polymer*, **41**, 5471 (2000).
(37) S.-H. Lim, A. Dasari, G.-T. Wang, Z.-Z. Yu, Y.-W. Mai, Q. Yuan, S. Liu, and M. S. Yong, *Compos. Part B*, **41**, 67 (2010).